The effect of anion fluorination in ionic liquids—physical properties of a range of bis(methanesulfonyl)amide salts

Jennifer M. Pringle,*[a] Jake Golding,[b] Krisztian Baranyai,[a] Craig M. Forsyth,[a] Glen B. Deacon,[a] Janet L. Scott[a] and Douglas R. MacFarlane[a]

[a] *Centre for Green Chemistry, School of Chemistry, Monash University, Clayton, Victoria 3800, Australia. E-mail: j.pringle@sci.monash.edu.au; Fax: (+613) 9905 4597; Tel: (+613) 9905 4535*

[b] *CSIRO Manufacturing and Infrastructure Technology, Private Bag 33, Clayton South MDC, Victoria 3169, Australia*

Received (in Montpellier, France) 11th April 2003, Accepted 21st May 2003
First published as an Advance Article on the web 28th August 2003

The bis(trifluoromethanesulfonyl)amide, TFSA, anion is widely used in the genesis of room temperature ionic liquids as it is non-spherical, fluorinated and has a particularly diffuse charge. However, the extent to which each of these structural features is responsible for the low melting point, fluidity and excellent stability of the resultant ionic liquids has yet to be described. We present the synthesis and analysis of a range of analogous, non-fluorinated species containing the bis(methanesulfonyl)amide, $NMes_2^-$, ligand. Utilisation of this anion produces ionic liquids that are hydrophilic and extremely low melting, but with decreased thermal and electrical stability and significantly increased viscosity. The crystal structures of the dimethyl pyrrolidinium bis(methanesulfonyl)amide and TFSA species are compared, and the number of close contacts within each is assessed. Comparison of these structural and physical properties provides new insight into the effect of anion fluorination on these ionic liquids.

Introduction

In the investigation of new anions for use in ionic liquids, for application both as solvents and in electrochemical devices, it has become apparent that the bis(trifluoromethanesulfonyl)-amide anion gives ionic liquids with substantially lower melting points and higher fluidity than almost any other anion. Additionally, the organic salts of the bis(trifluoromethanesulfonyl)amide anion are generally hydrophobic and are characteristically extremely stable, both thermally and electrochemically. Ionic liquids containing the bis(trifluoromethanesulfonyl)amide (TFSA) anion were first reported by Koch *et al.*[1] and, shortly after, by Bonhôte *et al.*[2] Since then, this species of ionic liquid has proven particularly popular for a range of applications.[3]

The TFSA anion combines a number of structural features to give the resultant salts their advantageous physical properties. The charge on the TFSA anion is particularly diffuse, spread through the S–N–S core and partially to the trifluoromethane groups, and this diffusivity results in a decreased interaction between the cation and the anion compared to ionic compounds with more localised anion charges, such as the halides. This is an important factor in reducing the melting point of the ionic liquid.[2] There is a complex, but poorly understood, relationship between anion and cation size, degree of interaction (both ionic and hydrogen bonding), packing, *etc.* that relates the physical properties of ionic liquids to their chemical structure. In an effort to enhance the understanding of such physico-chemical effects and in a continued drive to make and assess new ionic liquids, we report the synthesis of a range of novel ionic liquids of the bis(methanesulfonyl)amide anion ($NMes_2$). It was proposed that these species would exhibit the same favourable physical properties of the analogous TFSA species – good thermal and electrochemical stability *etc.* – but also have the additional advantage (for selected applications) of being hydrophilic and lower melting. In addition they would provide an insight into the effect of anion fluorination.

Experimental

General

Unless stated otherwise, chemicals were used as received (Sigma-Aldrich). The solvents (BDH) were dried over baked-out 3 Å molecular sieves.

Differential Scanning Calorimetry (DSC) was carried out on a Perkin-Elmer DSC-7 calibrated with cyclohexane (−86 and 6.54 °C) and *p*-nitrotoluene (51.64 °C). ^{1}H and ^{13}C NMR spectra were recorded at 300 MHz and 75 MHz respectively on a Bruker DPX-300 MHz spectrometer, in d_6-DMSO with tetramethylsilane as an internal standard.

Infrared spectra were recorded on a Perkin-Elmer FTIR 1600 instrument. Solid samples were examined as KBr discs ~5% w/w, while liquid samples were examined between sodium chloride plates.

Positive and negative electrospray mass spectroscopy was carried out on a Micromass Platform with an electrospray source. Samples were dissolved in a 1:1 methanol–water mixture. Viscosity was measured using an ASTM Kinematic viscometer size 500 inside a nitrogen dry box, at ambient temperature (23 °C) (flow times were in the order of minutes, hence uncertainties in time measurements were negligible). Density was measured by duplicated weighing of 2 mL, measured precisely using a microsyringe, of rigorously dried samples, using a balance accurate to four decimal places.

Cyclic voltammograms were recorded under a nitrogen atmosphere in a nitrogen dry box using a Maclab potentiostat,

 DOI: 10.1039/b304072k

and Maclab software. Electrodes consisted of a glassy carbon working electrode, a platinum wire counter electrode and a silver wire pseudo-reference electrode. Samples were dried for several hours under vacuum at < 0.1 atm, 50 °C before analysis.

Conductivity was measured using a locally designed multi-sample conductance cell consisting of a block of aluminium into which sample compartments were drilled. The cell constants of each compartment were determined using 0.01 M KCl at 25 °C and were approximately 1. The temperature was determined using a thermocouple and heating probe set into the aluminium block and connected to a Shimaden digital temperature controller. The conductivities were measured using AC Impedance spectroscopy between 20 Hz and 1 MHz on an HP4284A impedance meter. The conductance of the samples was determined from the real axis touchdown in the Nyquist plot.

The gas solubility measurements were made with a gravimetric microbalance (Cahn C-1000 Recording Balance) contained within a sample chamber and interfaced to a 166 MHz IBM PC *via* a DAC 220 analog to digital converter card. The weight range, sensitivity and sampling rate used in these experiments was 10 mg, 50 μg and 1 Hz respectively. The carbon dioxide was of food grade purity, 99.95%, purchased from BOC gases. The samples were dried and degassed thoroughly to a constant weight before use. The low solubility of CO_2 (discussed below) is testament to the purity of the ionic liquid, as the presence of the $(CH_3SO_2)_2NH$ or $CH_3SO_2NH_2$ starting materials would greatly increase the CO_2 solubility.

X-Ray crystallography

Data for single crystal structure analysis was measured on Nonius Kappa CCD using MoKα radiation ($\lambda = 0.71073$ Å) at $T = 123(2)$ K. Structure solution and refinement was achieved using the programs SHELXS-97[4] and SHELXL-97[5] respectively. Thermogravimetric analysis (TGA) was performed using an STA 1500 Rheometer Scientific, calibrated with indium, tin, lead and zinc, under a nitrogen atmosphere at a heating rate of 10 °C min^{-1}. †

Crystal data for $P_{11}(NMes_2)$. $C_8H_{20}N_2O_4S_2$, $M = 272.38$, colourless prismatic, $0.075 \times 0.30 \times 0.30$ mm^3, monoclinic, space group $P2_1/n$ (No. 14), $a = 8.2308(1)$, $b = 10.5652(1)$, $c = 14.6405(2)$ Å, $\beta = 95.159(1)°$, $V = 1268.0(4)$ Å^3, $Z = 4$, $D_c = 1.427$ g/cm^3, $F_{000} = 584$, $2\theta_{max} = 56.6°$, 18 383 reflections collected, 3104 unique ($R_{int} = 0.0429$). Final $GooF = 1.089$, $R1 = 0.0308$, $wR2 = 0.0778$, R indices based on 2477 reflections with $I > 2\sigma(I)$ (refinement on F^2), 225 parameters, 0 restraints. Lp and absorption corrections applied, $\mu = 0.422$ mm^{-1}.

Synthesis and characterisation

Synthesis of the iodide salts of the imidazolium, tetraalkylammonium and pyrrolidinium cations has been reported previously.[6,7] For consistency the abbreviations previously used to describe the pyrrolidinium and ammonium cation are used here, where P = pyrrolidinium and N = ammonium, with a subscript to indicate the number of carbons in the linear alkyl chain substituent (Scheme 1), emi indicates the 1-ethyl-3-methylimidazolium cation. For simplicity the bis(methanesulfonyl)imide anion is referred to as $NMes_2$, to indicate its structure in terms of two mesylate moieties bonded to a nitrogen atom. This is similar nomenclature to that used by Bonhôte *et al.*,[2] who abreviate the TFSA anion as NTf_2, where Tf indicates the triflate moiety.

† CCDC reference number 210766. See http://www.rsc.org/suppdata/nj/b3/b304072k/ for crystallographic files in CIF or other electronic format.

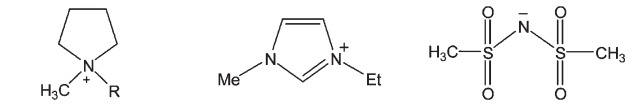

Scheme 1 The chemical structures of the pyrrolidinium, imidazolium and bis(methanesulfonyl)amide ions.

Bis(methanesulfonyl)amine ($HNMes_2$ 1). $CH_3SO_2NH_2$ (22.0 g, 0.231 mol) and KOH (25.956 g, 0.462 mol) were added together in water and cooled to 0 °C. CH_3SO_2Cl (18 ml, 0.231 mol) was added dropwise and the stirred solution warmed slowly to room temperature and stirred for 5 h. The solution was then acidified with HCl and cooled overnight, producing a white precipitate, which was removed by filtration and washed with diethyl ether. Recrystalisation from acetone gave the product as a white solid, yield 31.9 g, 80%, mp 150 °C. (lit. mp = 152–155 °C).[9] IR (KBr): 3275.9 s, 2665 w, 1637 w, 1578 w, 1328 s [γ(SO_2)], 1155 s [ν(SO_2)], 986 s, 918 s, 884 s, 768 s, 531 s, 500 s cm^{-1}. ^{1}H NMR (300 MHz, D_2O): δ (ppm) 3.0, s, CH_3. ES-MS; ES^- m/z 171.9, 100% $[(CH_3SO_2)_2N]^-$.

Conversion of the halide salts to the desired bis(methanesulfonyl)amide salts was effected by reaction with silver hydroxide, prepared by reaction of $AgNO_3$ and 1 M NaOH solution. The precipitated AgOH was washed thoroughly to remove any residual salts then added to an aqueous solution of the halide salt. The solution was stirred for 1 h and the precipitated solid (AgI and excess AgOH) filtered off. An equimolar amount of bis(methanesulfonyl)amine $(CH_3SO_2)_2NH$ was added to the aqueous solution of the cat^+OH^- to effect the metathesis to the $NMes_2$ species. This synthetic technique is particularly advantageous as the end point of the metathesis can be easily detected by pH measurement, which ensures the absence of any unreacted acid or hydroxide ionic liquid. The water was then removed by evaporation under vacuum. Repeated addition of dichloromethane or chloroform, followed by cooling to *ca.* −10 °C for 48 h and filtration through glass fibre filter paper to remove any precipitated silver salts, was performed to ensure the remove of any silver species, as confirmed by mass spectrometry. The absence of organic impurities was confirmed by ^{1}H and ^{13}C NMR and IR. All samples were dried for several hours under vacuum at < 0.1 atm, 50 °C and the absence of water confirmed by TGA analysis, which showed no weight loss from the samples below at least 250 °C. All of the $NMes_2$ ionic liquids prepared were fully miscibile with water.

***N*,*N*-dimethylpyrrolidinium bis(methanesulfonyl)amide ($P_{11}NMes_2$, 2).** $AgNO_3$ (1.94 g, 11.4 mmol, converted to AgOH by reaction with 1 M NaOH solution), $P_{11}I$ (2.16 g, 9.5 mmol) and $HN(SO_2CH_3)_2$ (1.64 g, 9.5 mmol) gave **2** as a colourless solid (2.46 g, 95% yield, m.p. 40–55 °C). IR (KBr): 3530 s br, 3029 m, 2976 m, 2936 m [δ(C–H)], 2087 w br, 1875 w br, 1752 w br, 1645 m br, 1478 s br [γ(C–H)], 1421 m br, 1320 m br, 1268 s br [ν (SO_2)], 1141 s [ν (SO_2)], 1106 s [ν (SO_2)], 1058 s, 957 s, 819 s, 782 s cm^{-1}. ^{1}H NMR (300 MHz, DMSO-d_6): δ (ppm) 2.1, m, 4H, $2CH_2$ (ring); 2.7, s, 6H, $2SO_2$–CH_3; 3.1, s, 6H, 2N–CH_3; 3.5, t, 4H, $2CH_2$ (ring). ^{13}C NMR (75 MHz, DMSO-d_6): δ (ppm) 21.3, CH_2; 40.0, SO_2CH_3; 50.9, CH_3; 64.7, CH_2 (ring). ES-MS: ES^+ m/z 372.3, 5% $[[P_{11}]_2^+[(CH_3SO_2)_2N^-]]^+$; 99.8, 100% $[P_{11}]^+$. ES^- m/z 171.8, 100% $[(CH_3SO_2)_2N]^-$.

***N*-methyl-*N*-ethyl-pyrrolidinium bis(methanesulfonyl)amide ($P_{12}NMes_2$, 3).** $AgNO_3$ (1.94 g, 11.4 mmol, converted to AgOH), $P_{12}I$ (2.29 g, 9.5 mmol) and $HN(SO_2CH_3)_2$ (1.64 g,

9.5 mmol) gave **3** as a colourless liquid (2.51 g, 92% yield). IR (neat liquid): 3534 s br, 3026 m [ν(C–H)], 2986 m [ν(C–H)], 1873 w br, 1750 w br, 1648 m br, 1472 m br [ν(C–H)], 1425 w, 1318 m s, 1269 s [ν(SO_2)], 1140 m [ν(SO_2)], 1106 s [ν(SO_2)], 1057 s, 955 m, 818 s, 761 s cm^{-1}. ^1H NMR (300 MHz, DMSO-d_6): δ (ppm) 1.3, t, 3H, CH_3; 2.1, m, 4H, $2CH_2$ (ring); 2.7, s, 6H, $2SO_2$–CH_3; 3.0, s, 3H, CH_3; 3.4, q, 2H, CH_2; 3.5, m, 4H, $2CH_2$ (ring). ^{13}C NMR (75 MHz, DMSO-d_6): δ (ppm) 8.7, CH_3; 21.0, $2CH_2$ (ring); 39.5, SO_2–CH_3; 46.9, CH_3; 58.3, $2CH_2$ (ring); 62.9, CH_2. ES-MS; ES^+ m/z 400.3, 5% $[[P_{12}^+]_2[(CH_3SO_2)_2N^-]]^+$; 100% $[P_{12}]^+$. ES^- m/z 458.1, 20% $[[P_{12}]^+[(CH_3SO_2)_2N^-]_2]^-$; 171.9, 100% $[(CH_3SO_2)_2N]^-$.

***N*-methyl-*N*-propyl-pyrrolidinium bis(methanesulfonyl)amide ($P_{13}NMes_2$, 4).** $AgNO_3$ (1.94 g, 11.4 mmol, converted to AgOH), $P_{13}I$ (2.42 g, 9.5 mmol) and $HN(SO_2CH_3)_2$ (1.64 g, 9.5 mmol) gave **4** as a colourless liquid (2.57 g, 90% yield). IR (neat liquid): 3554 s br, 3281 m, 3025 s [ν(C–H)], 2974 s [ν(C–H)], 2884 s [ν(C–H)], 2360, 1869 m, 1749 m, 1647 m, 1474 s [ν(C–H)], 1424 m, 1316 s, 1271 s [ν(SO_2)], 1139 s [ν(SO_2)], 1107 s [ν(SO_2)], 1053 s, 953 s, 817 s, 758 s, 695 m cm^{-1}. ^1H NMR (300 MHz, DMSO-d_6): δ (ppm) 0.9, t, 3H, CH_3; 1.7, m, 2H, CH_2; 2.1, m, 4H, $2CH_2$ (ring); 2.7, s, 6H, $2SO_2$–CH_3; 3.0, s, 3H, CH_3; 3.3, m, 2H, CH_2; 3.4, m, 4H, $2CH_2$ (ring). ^{13}C NMR (75 MHz, DMSO-d_6): δ (ppm) 10.6, CH_3; 16.5, CH_2; 21.0, $2CH_2$ (ring); 42.0, SO_2–CH_3; 47.5, CH_3; 63.4, CH_2 (ring); 64.4, CH_2. ES-MS; ES^+ m/z 428.3, 5% $[[P_{13}]_2^+[(CH_3SO_2)N]^-]^+$; 127.8, 100% $[P_{13}]^+$. ES^- m/z 474.1, 5% $[[P_{13}]^+[(CH_3SO_2)_2N^-]_2]^-$; 171.8, 100% $[(CH_3SO_2)_2N]^-$.

***N*-methyl-*N*-butyl-pyrrolidinium bis(methanesulfonyl)amide ($P_{14}NMes_2$, 5).** $AgNO_3$ (1.94 g, 11.4 mmol, converted to AgOH), $P_{14}I$ (2.55 g, 9.5 mmol) and $HN(SO_2CH_3)_2$ (1.64 g, 9.5 mmol) gave **5** as a colourless liquid (2.75 g, 92% yield). IR (neat liquid) 3554 s br, 3025 m [ν(C–H)], 2964 s [ν(C–H)], 2877 m, 1870 w, 1750 w, 1637 w, 1468 m [ν(C–H)], 1424 w, 1315 m, 1271 s [ν(SO_2)], 1139 m [ν(SO_2)], 1107 s [ν(SO_2)], 1053 s, 954 m, 817 m, 758 m, 695 cm^{-1}. ^1H NMR (300 MHz, DMSO-d_6): δ (ppm) 0.9, t, 3H, CH_3; 1.3, m, 2H, CH_2; 1.7, m, 2H, CH_2; 2.1, m, 4H, $2CH_2$ (ring); 2.7, s, 6H, $2SO_2$–CH_3; 3.0, s, 3H, CH_3; 3.3, m, 2H, CH_2; 3.5, m, 4H, $2CH_2$ (ring). ^{13}C NMR (75 MHz, DMSO-d_6): δ (ppm) 13.4, CH_3; 19.2, CH_2; 21.0, $2CH_2$ (ring); 24.8, CH_2; 42.1, SO_2–CH_3; 47.5, CH_3; 62.9 $2CH_2$ (ring); 63.3, CH_2. ES-MS; ES^+ m/z 456.3, 8% $[[P_{14}]_2^+[(CH_3SO_2)N]^-]^+$; 141.9, 100% $[P_{14}]^+$. ES^- m/z 486.1, 20% $[[P_{14}]^+[(CH_3SO_2)_2N^-]_2]^-$; 171.9, 100% $[(CH_3SO_2)_2N]^-$.

***N*-methyl-*N*-hexyl-pyrrolidinium bis(methanesulfonyl)amide ($P_{16}NMes_2$, 6).** $AgNO_3$ (1.94 g, 11.4 mmol, converted to AgOH), $P_{16}I$ (2.82 g, 9.5 mmol) and $HN(SO_2CH_3)_2$ (1.64 g, 9.5 mmol) gave **6** as a colourless liquid (2.86 g, 88% yield). IR (neat liquid) 3568 m br, 3025 m [ν(C–H)], 2932 s [ν(C–H)], 2860 m, 1870 m, 1749 m, 1654 m, 1469 m [ν(C–H)], 1424, 1379, 1355, 1315, 1272 s [ν(SO_2)], 1140 m, [ν(SO_2)], 1108 s, [ν(SO_2)], 1055 s, 956 m, 817 s, 759 s, 695 m cm^{-1}. ^1H NMR (300 MHz, DMSO-d_6): δ (ppm) 0.9, t, 3H, CH_3; 1.3, m, 6H, $3CH_2$; 1.7, m, 2H, CH_2; 2.1, m, 4H, $2CH_2$; 2.8, s, 6H, $2SO_2$–CH_3; 3.0, s, 3H, CH_3; 3.3, m, 2H, CH_2; 3.4, m, 4H, $2CH_2$ (ring). ^{13}C NMR (75 MHz, DMSO-d_6): δ (ppm) 13.2, CH_3; 20.5, CH_2; 21.3, $2CH_2$ (ring); 22.3, CH_2; 25.0, CH_2; 30.1, CH_2; 41.6, SO_2–CH_3; 47.0, CH_3; 62.5, $2CH_2$ (ring); 62.9, CH_2. ES-MS; ES^+ m/z 512.3, 7% $[[P_{16}]_2^+[(CH_3SO_2)N]^-]^+$; 170.0, 100% $[P_{16}]^+$. ES^- m/z 514.1, 10% $[[P_{16}]^+[(CH_3SO_2)_2N^-]_2]^-$; 171.8, 100% $[(CH_3SO_2)_2N]^-$.

N-hexyl-*N*,*N*,*N*-triethylammonium bis(methanesulfonyl)amide ($N_{6222}NMes_2$, 7). $AgNO_3$ (1.94 g, 11.4 mmol, converted to AgOH), $N_{6222}I$ (2.98 g, 9.5 mmol) and $HN(SO_2CH_3)_2$ (1.64 g, 9.5 mmol) gave **7** as a colourless liquid (2.89 g, 85% yield). IR (neat liquid) 3554 m br, 2955 s [ν(C–H)], 2932 s [ν(C–H)], 2861 m, 1868.7 w, 1750 w, 1646 w, 1460 m [ν(C–H)], 1397 m, 1313 m, 1272 s [ν(SO_2)], 1140 m [ν(SO_2)], 1109 m [ν(SO_2)], 1056 s, 955 m, 816 s, 758 s, 695 w cm^{-1}. ^1H NMR (300 MHz, DMSO-d_6): δ (ppm) 0.9, t, 3H, CH_3; 1.2, t, 9H, $3CH_3$; 1.3, m, 6H, $3CH_2$; 1.6, m, 2H, CH_2; 2.7, s, 6H, $2SO_2$–CH_3; 3.1, m, 2H, N–CH_2; 3.2, 6H, 3N–CH_2. ^{13}C NMR (75 MHz, DMSO-d_6): δ (ppm) 7.1, $3CH_3$; 13.7, CH_3; 20.8, CH_2; 21.8, CH_2; 25.4, CH_2; 30.6, CH_2; 42.1, SO_2–CH_3; 51.9, 3N–CH_2; 56.0, N–CH_2. ES-MS; ES^+ m/z 544.4, 10% $[N_{6222}]_2^+[(CH_3SO_2)_2N^-]$; 186.1, 100% $[N_{6222}]^+$. ES^- m/z 530.2, 30% $[N_{6222}]^+[(CH_3SO_2)_2N^-]_2$); 171.9, 100% $[(CH_3SO_2)_2N]^-$.

***N*-hexyl-*N*,*N*,*N*-tributylammonium bis(methanesulfonyl)amide ($N_{6444}NMes_2$, 8).** $AgNO_3$ (1.94 g, 11.4 mmol, converted to AgOH), $N_{6444}I$ (3.78 g, 9.5 mmol) and $HN(SO_2CH_3)_2$ (1.64 g, 9.5 mmol) gave **8** as a colourless liquid (3.78 g, 90% yield). IR (neat liquid) 3568 m, 2960 s [ν(SO_2)], 2875 s [ν(C–H)], 1869 m, 1747 m, 1637 m, 1470 s [ν(C–H)], 1312 m, 1275 s [ν(SO_2)], 1140 s [ν(SO_2)], 1110 s [ν(SO_2)], 1055 s, 956 s, 816 s, 757 s cm^{-1}. ^1H NMR (300 MHz, DMSO-d_6): δ (ppm) 0.9, m, 12H, $4CH_3$; 1.3, m, 12H, 6 CH_2; 1.6, m, 8H, $4CH_2$; 2.7, s, 6H, $2SO_2$–CH_3; 3.2, m, 8H, 4N–CH_2. ^{13}C NMR (75 MHz, DMSO-d_6): δ (ppm) 13.4, $3CH_3$; 13.7, CH_3; 19.1, $3CH_2$; 20.9, CH_2; 21.8, CH_2; 23.0, $3CH_2$; 25.4, CH_2; 30.5, CH_2; 42.1, SO_2–CH_3; 57.5, 3N–CH_2; 57.9, N–CH_2. ES-MS; ES^+ m/z 270.4, 100% $[N_{6444}]^+$. ES^- m/z 614.2, 30% $[N_{6444}^+][(CH_3SO_2)_2N^-]_2$, 171.9, 100% $[(CH_3SO_2)_2N]^-$.

1-ethyl-3-methylimidazolium bis(methanesulfonyl)amide ($emiNMes_2$, 9). $AgNO_3$ (10.0 g, 58.8 mmol, converted to AgOH), emiI (12.73 g, 53.5 mmol) and $HN(SO_2CH_3)_2$ (9.26 g, 53.5 mmol) gave **9** as a colourless liquid (14.38 g, 95% yield). IR (neat liquid) 3550 s, 3153 s [ν (C–H)], 3110 s [ν(C–H)], 1872 w, 1749 w, 1644 w, 1573.9 s, 1455 m, 1424 m, 1319 m, 1270 s [ν(SO_2)], 1171 s [ν(SO_2)], 1107 s [ν(SO_2)], 1055 s, 956 m, 818 s, 760 s 698 m, 648 m, 624 m cm^{-1}. ^1H NMR (300 MHz, DMSO-d_6): δ (ppm) 1.4, t, 3H, CH_3; 2.7, s, 6H, $2SO_2$–CH_3; 3.8 s, 3H, N–CH_3; 4.1, m, 2H, CH_2; 7.6, m, 1H, CH; 7.7, m, 1H, CH; 9.0, s, 1H, NCHN. ES-MS; ES^+ m/z 110.8, 100% $[emi]^+$. ES^- m/z 452.9, 40% $[emi^+][(CH_3SO_2)_2N^-]_2$; 171.7, 100% $[(CH_3SO_2)_2N]^-$.

Results and discussion

Structural and physical properties

Synthesis of bis(methansulfonyl)amine was described in 1940 by Helferich and Grünert,[8] who reported its strongly acidic nature. The melting points of the acid and the aniline salt of a range of disulfonylamides, including the $HNMes_2$ species, were documented by Runge *et al.*[9] in 1955. The potential of this anion, when used in combination with a quaternary ammonium cation, was explored by Blaschette *et al.*,[10] who report the synthesis and physical properties of a range of tetraalkylammonium bis(methanesulfonyl)amide salts, identified as a useful source of free $(CH_3SO_2)_2N^-$ ions when dissolved in low polarity solvents. The melting points reported for the Et_4N and Pr_4N $NMes_2$ salts are lower than those of the TFSA analogues synthesised within our group,[11] which indicates a potential source of low melting point ionic liquids. This, and the importance of assessing the effect of anion fluorination on the physical properties of ionic liquids, led us to the synthesis and physical characterisation of the range of $NMes_2$ ionic liquids reported here.

Hydrogen bonding within ionic liquids is relatively poorly understood, and has been the subject of a number of

investigations.[12] The chemical shift of the C(2)–H proton of the imidazolium cation in ionic liquids has been reported to be related to the extent of hydrogen bonding within the liquid, with a downfield shift occurring on increased hydrogen bonding.[2] While it is important to note that this may also be affected by factors such as concentration and cation–cation interactions, it is interesting to note that the chemical shift of the C(2)–H proton of the emi$NMes_2$ species is 9.45 ppm in $CDCl_3$, a considerable downfield shift from 8.8 ppm of the analogous TFSA species under the same conditions. This indication of significantly increased hydrogen bonding in the non-fluorinated species is consistent with our other observations, as detailed below, and with the water miscibility of the series.

The effect of anion fluorination on the thermal properties of the ionic liquids was investigated using differential scanning calorimetry (DSC). Typical DSC thermograms for the $NMes_2$ compounds are shown in Fig. 1. Data for the $NMes_2$ compounds prepared here are compared with the corresponding TFSA compounds, Table 1. The glass transition temperatures, evidenced in the thermograms, rise with increasing alkyl chain length within the *N*-alkyl-*N*-methylpyrrolidinium salt series. This trend is also seen in the tetraalkylammonium salts, although these are relativly low-energy transitions. The glass transition temperatures are all approximately 30 °C above those of the equivalent TFSA salts (Table 1).

The only melting point evidenced in the DSC thermograms was for the $P_{11}NMes_2$ salt, even when the samples were cooled very slowly to encourage crystallisation. The crystallisation can be seen as an exothermic transition in the DSC thermogram of the $P_{11}NMes_2$ salt at −10 °C, whereas there are no equivalent transitions in the thermograms of any of the other $NMes_2$ species. The dimethylpyrrolidinium salt melts over a broad temperature range, between 40 and 55 °C, which is considerably lower than that of the fluorinated analogue (132 °C).[21] Similarly, the $P_{12}NMes_2$ species is liquid at room temperature, whereas the P_{12}TFSA species melts at 86 °C. This is likely to be predominantly a result of the significantly lower mass of the anion in the non-fluorinated case (some 38% lower anion weight), which clearly overcomes the effects of any changes in the electrostatic interactions. In the absence of hydrogen bonding, this would also be reflected in a lower glass transition temperature. However, while the melting point of a species is sensitive to features that are present in both the liquid and solid states, such as molecular mass, the Tg is affected by the physical properties of the liquid only, *i.e.* increased hydrogen bonding, thus Tg rises. This explains the initially surprising result, that use of the non-fluorinated anion results in a simultaneous drop in melting point and rise in Tg. The different basicities of the anions can also be expected to play a role in determining the melting point of the species. The $HNMes_2$ species is a weaker acid (pK_a 2.85)[10] than bis(trifluoromethanesulfonyl)amine (pK_a = 1.7)[13] and thus forms a stronger conjugate base. This is expected to result in a greater degree of hydrogen bonding to the cation.

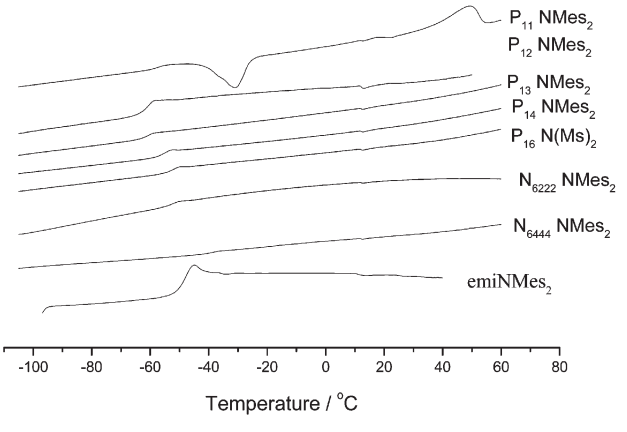

Fig. 1 DSC traces of the bis(methanesulfonyl)amide ionic liquids.

Table 1 Comparison of the glass transition temperatures of the fluorinated and non-fluorinated amide salts

	Tg/°C	
	$NMes_2$	TFSA[2,11,21]
P_{11}	−58	—
P_{12}	−64	−102
P_{13}	−63	−90
P_{14}	−58	−87
P_{16}	−55	−87
N_{6222}	−54	−81
N_{6444}	−42	−88
emi	−50	−95

The lower densities of the $NMes_2$ species (Table 2) reflect the fact that the molecular volume of the anions is similar but the mass of the fluorine is greater.

A particularly significant effect of loss of anion fluorination on the physical properties of these ionic liquids is the effect on the viscosity. A combination of very slightly decreased anion size, less diffuse charge and large increase in hydrogen bonding within the salts results in a surprisingly large increase in viscosity (Table 2). The significant changes in viscosity and glass transition temperature clearly indicate the significant influence of anion fluorination on the liquid state of these compounds. X-ray crystallographic analysis allows some assessment of the differences in the solid state, by comparison of the solid-state structures of $P_{11}NMes_2$ (Fig. 2) and P_{11}TFSA.[14] In both structures, the anion is in a *trans* configuration, but in the non-fluorinated species, the C–S–S–C torsion angle is reduced, from 173.4° to 147.4°. There is also a significant decrease (0.067 Å) in the S–C bond length in the absence of fluorination and other bond lengths reflect the electronegativity of the hydrogen *vs.* fluorine atoms. There is a small increase in the N–S and S–O bond lengths in the absence of fluorination for the same reason. These changes in bond lengths are consistent with those observed in the previously reported $[Me_2NH_2][N(SO_2CH_3)_2]$ structure, although in this complex the C–S–S–C torsion angle is further reduced, to just 130.7°.[15]

The more significant effect of anion fluorination within these species is its influence on the degree of interaction between the anion and the cation. This directly affects the melting point of the species—more cation–anion interaction would clearly be expected to increase the melting point. Both the dimethyl pyrrolidinium $NMes_2$ and TFSA structures show significant O–H interactions between the SO_2 groups of the anion and the hydrogen atoms of the cation, and both show one significant anion–cation N···H interaction (Tables 3 and 4 for the $NMes_2$ and TFSA species respectively). However, the difference in the two structures lies in the interactions to the CF_3 or CH_3 groups of the anion. In the TFSA structure, the CF_3 groups form an F···H–C interaction with neighbouring cations, where the donor is the C–H of the cation and the acceptor is the electronegative fluorine atom on the anion (shown in the first three entries in Table 4). However, in the $NMes_2$ structure, a

Table 2 Densities and viscosities of selected $NMes_2$ and TFSA ionic liquids

	Density/g mL^{-1}		Viscosity/cP (20 °C)	
Cation	$NMes_2$	TFSA	$NMes_2$	TFSA
P_{14}	1.280	1.41[21]	1680	85 (25 °C)
emi	1.343	1.520[2]	787	34

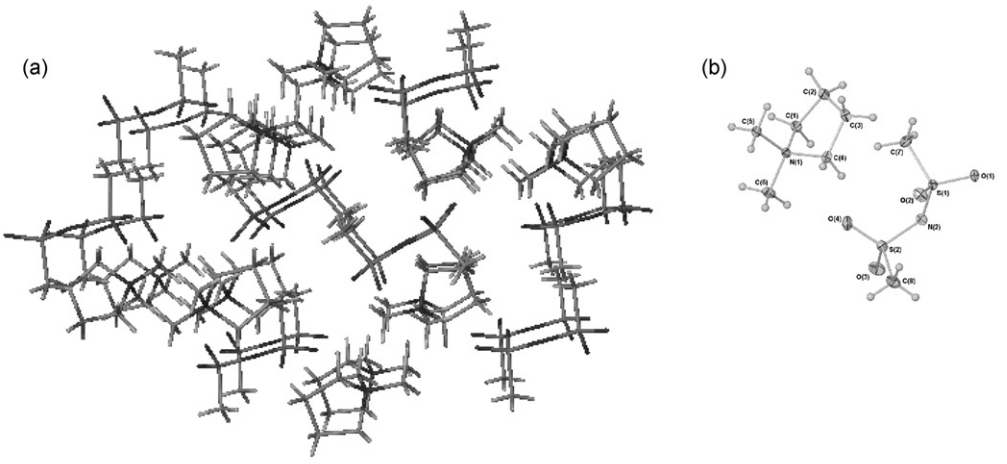

Fig. 2 The solid state structure of *N*,*N*-dimethylpyrrolidinium bis(methanesulfonyl)amide.

C–H···O interaction is present, where the donor is the C–H of the *anion*, and the acceptor is the electronegative oxygens of neighbouring anions (shown in the first two entries in Table 3). Thus, in the latter structure the hydrogen bonding gives rise to an attractive anion–anion interaction, as well as the cation–anion interactions. The shortest cation–anion N···N interaction distance (representing the distance between the nominal centres of positive and negative charge) within the TFSA structure is 4.54 Å compared to 4.02 Å in the $NMes_2$ structure. This is predominantly a reflection of the less diffuse anion charge in the latter species, which results in a greater charge on the nitrogen of the $NMes_2$ than in the TFSA species. Thus, despite the hydrogen bonding and stronger N···N interactions providing a stronger electrostatic interaction, the melting point of the $NMes_2$ species is still lower, suggesting that it is the lower mass of the anion that is the predominant effect.

Thermal and electrochemical properties

The thermal stability of the ionic liquids was assessed using rising temperature thermogravimetric analysis (TGA). The TFSA ionic liquids are known to be particularly thermally stable, so assessment of the importance of anion fluorination to this thermal stability was deemed of particular interest. The thermal stability of the species also has important ramifications in determining any possible applications of the $NMes_2$ ionic liquids. The TGA plots for representative $NMes_2$ and TFSA salts are shown in Fig. 3.

Thermal analysis shows that in the absence of anion fluorination the thermal stability of the ionic liquids is significantly reduced. The pyrrolidinium and imidazolium $NMes_2$ species are approximately 150 °C less stable than the TFSA analogues. This is a reflection of the chemical stability of the species (in this case, how readily volatile degradants are formed) as opposed to the melting point, which is a reflection of the strength of the attractive forces between the molecules. Significantly, both the melting point and the thermal stability are lower in the non-fluorinated species.

The thermal stability of the $NMes_2$ tetraalkylammonium salts was reported by Blaschette *et al.* in their original publication.[10] They observed alkyl transfer from the tetraalkylammonium cation at temperatures ranging from 200 to 250 °C, with the thermal stability depending on the nature of the cation ($Bu_4N > Et_4N > Me_4N > MeEt_3N$). This is slightly lower than the decomposition temperatures observed for the ionic liquids reported here. Our investigations have found that the heavier $HexBu_3N$ species is thermally stable to *ca.* 275 °C (Fig. 3, middle trace), and the imidazolium and pyrrolidinium species are even more stable. Analysis of the decomposition products of $emiNMes_2$ by pyrolysis mass spectroscopy at 300 °C show the presence of $MeN(SO_2CH_3)_2$ and $EtN(SO_2CH_3)_2$, probably formed by alkyl transfer. The analogous products are not observed in the emiTFSA spectrum at 300 °C, but are observed when the pyrolysis temperature is increased to 700 °C. This is discussed further in a separate publication.[16] In addition to being less thermally stable, the $NMes_2$ species were also observed to be less electrochemically stable than the TFSA analogues (Table 5). The electrochemical stability of the non-fluorinated anion is lower, with oxidation of the $NMes_2$ anion occurring approximately 1 V lower in potential than for the TFSA anion. The nature of the anion can also affect the electrochemical stability of the cation, as evidenced here, with a further 0.5 to 1 V increase in the reduction potential of the cation. Both cyclic voltammograms are featureless

Table 3 Distances and angles of the close contacts within the *N*,*N*-dimethyl pyrrolidinium bis(methanesulfonyl)amide structure

D–H···A	Distance (H···A)/Å	Distance (D···A)/Å	Bond Angle (DHA)/°
C(7)–H(7C)···O(1)[a]	2.58(2)	3.121(2)	116(1)
C(7)–H(7A)···O(3)[a]	2.68(2)	3.599(2)	171(2)
C(5)–H(5A)···O(2)	2.36(2)	3.232(2)	154(1)
C(1)–H(1B)···O(1)	2.56(2)	3.062(2)	111(1)
C(6)–H(6B)···O(3)	2.57(2)	3.465(2)	158(1)
C(2)–H(2A)···O(2)	2.63(2)	3.504(2)	151(1)
C(6)–H(6C)···O(1)	2.70(2)	3.049(2)	101(1)
C(5)–H(5C)···O(3)	2.69(2)	3.570(2)	152(1)
C(4)–H(4A)···N(2)	2.50(2)	3.422(2)	162(1)

D = donor, A = acceptor.[a] anion–anion interactions.

Table 4 Distances and angles of the close contacts within the *N*,*N*-dimethyl pyrrolidinium bis(trifluoromethanesulfonyl) amide structure, calculated from the crystallographic data published by Forsyth *et al.*[14] All interactions are cation–anion

D–H···A	Distance (H···A)/Å	Distance (D···A)/Å	Bond Angle (DHA)/°
C(4)–H(4B)···F(4)	2.58(2)	3.434(2)	147(2)
C(3)–H(3A)···F(6)	2.64(3)	3.594(3)	173.0(2)
C(2)–H(2B)···F(5)	2.63(3)	3.501(3)	167.0(2)
C(3)–H(5C)···O(3)	2.66(2)	3.507(3)	153(2)
C(6)–H(6B)···O(1)	2.64(2)	2.934(3)	109(2)
C(4)–H(4B)···O(4)	2.65(2)	3.450(3)	142(2)
C(1)–H(1A)···O(2)	2.31(2)	3.199(2)	161(2)
C(6)–H(6A)···O(3)	2.42(2)	3.324(3)	161(2)
C(5)–H(5A)···N(2)	2.64(2)	3.557(3)	159(2)

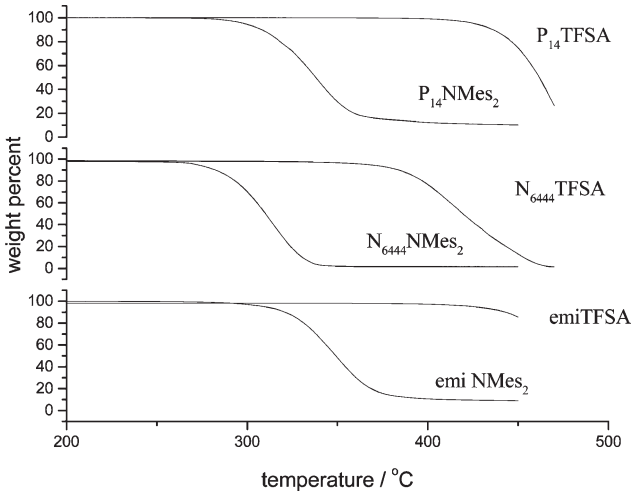

Fig. 3 TGA traces of three $NMes_2$ and TFSA salts.

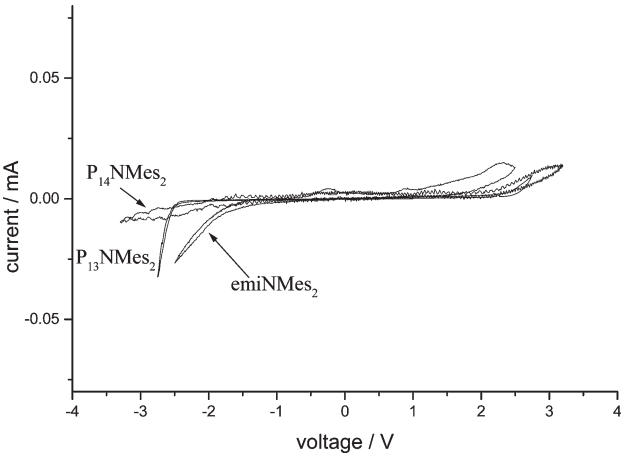

Fig. 4 Cyclic voltammograms of the $NMes_2$ salts.

between the oxidation and reduction limits (Fig. 4). As observed for the TFSA and other ionic liquids, the imidazolium cation is less electrochemically stable than the pyrrolidinium or tetraalkylammonium species. The electrochemical window of the latter two species, although smaller than that of the TFSA series, is still in excess of 4 V—large enough for a wide range of electrochemical applications.

If the applicability of the Stokes–Einstein equation to ionic liquids is assumed, the conductivity of an ionic liquid is predicted to be directly proportional to its density and inversely proportional to its formula weight and viscosity.[2,17] On changing to the non-fluorinated anion, the conductivity drops considerably. Thus, the decrease in density and the large increase in viscosity overshadow the decrease in formula weight, which should be beneficial to the conductivity. The applicability of the Stokes–Einstein equation to ionic liquids has been questioned,[18] however, in this context, for the empirical comparison of two different ionic liquid species it is believed that this treatment is valid.

This relationship between viscosity and conductivity of a liquid is the basis of the Walden rule. This has recently been discussed in the context of ionic liquids by Angell *et al.*,[19] who showed that many ionic liquids lie on what is described as an "ideal" Walden product line on a plot of log equivalent conductivity *vs.* log inverse viscosity. This is also true, at room temperature, for the two systems studied here. Angell *et al.* have also investigated the dependance of the cohesion of the salts, indicated by the glass transition temperature, and the molar volumes, of a range of ionic liquids and it is interesting to note that the $NMes_2$ species that we report show a significant deviation from the general trend that they observed. This again serves to emphasise the over-riding effect that hydrogen bonding has on the glass transition temperature of these systems.

Table 5 The effect of anion fluorination on the electrochemical properties of the ionic liquids

Cation	Electrochemical window/V		Conductivity/ mS cm^{-1} (25 °C)	
	$NMes_2$	TFSA	$NMes_2$	TFSA
P_{13}	−2.25 to +2			
P_{14}	−2 to +2	−3 to +3[21]	0.07	2.2[21]
Emi	−1.5 to +1	−2 to +2.5[2]	0.17	8.8 (20 °C^2)
N_{6444}	−3 to +2		0.005	0.16[11]
N_{6222}		−3 to +3		

The effect of anion fluorination on the physical properties of these ionic liquids was further explored by measuring the solubility of carbon dioxide in the two imidazolium-based species. The gas absorption capability of an ionic liquid is of interest in some potential applications of these species. A large percentage of synthetic reactions, such as hydrogenation, oxidation *etc.*, involve the use of dissolved gases, and the solubility of these gases may be the rate limiting factor in these reactions.

Gas absorption studies show a relatively high solubility of CO_2 in both ionic liquids, with Henry's Law constants of 76 ± 8 atm for $emiNMes_2$ and 47 ± 6 atm for the emiTFSA species at 20 °C. These values are comparable to those of Anthony *et al.*,[20] who report a Henry's Law constant of 53.4 ± 0.3 bar ($\equiv 52.7 \pm 0.3$ atm) for CO_2 in $bmimPF_6$ at 25 °C (NB: a low Henry's law constant indicates high gas absorption). Interestingly, it is clear that the CO_2 absorption capability of the ionic liquid decreases in the absence of anion fluorination. The solubility of a gas is governed by a combination of the polarisability of the gas and the dispersion forces and chemical interactions between the gas and the solvent. The relative influence of each of these factors differs with the nature of the gas and the solvent involved. The increased solubility of CO_2 in the TFSA ionic liquid compared to the $NMes_2$ species is postulated to be a reflection of a greater interaction between the CO_2 and the TFSA anion.[20] CO_2 has a large quadrupole moment and therefore dissolution may be more energetically favourable in a solvent where the anion charge is more diffuse. This also has important implications in the potential applications of these ionic liquids, as the hydrogen bonding in the $NMes_2$ series may enable the dissolution of a variety of inorganic and organic compounds that are insoluble in the TFSA series.

Conclusions

Utilisation of the bis(methanesulfonyl)amide anion yields a particularly low melting, hydrophilic, glass forming series of ionic liquids. This anion produces a significant increase in hydrogen bonding, as evidenced by a significant rise in the glass transition temperature and a concurrent increase in viscosity. This, in turn, produces a significant drop in conductivity. The lack of anion fluorination also results in a decrease in thermal and electrochemical stability of the corresponding salts. Analysis of the crystal structure of the dimethyl pyrrolidinium salts reveals anion–anion close contacts not present in the TFSA structure, in addition to a significantly shorter cation–anion N···N distance. The diffuse nature of the charge on the TFSA anion is commonly cited as the reason for the low melting point of these ionic liquids. However, the effect of a

more localised charge in the absence of fluorination, is overshadowed by the lower molecular mass of the $NMes_2$ anion. This results in a decrease in the melting point of the dimethyl pyrrolidinium salt. The low melting point and significant hydrogen bonding in this series, which may allow the dissolution of a range of hydrophilic inorganic and organic species, may prove the $NMes_2$ series particularly valuable perhaps at higher temperatures for a number of applications for which the TFSA series is unsuitable.

References

1 V. R. Koch, C. Nanjundiah, G. Battista Appetecchi and B. Scrosati, *J. Electrochem. Soc.*, 1995, **142**(7), L116–L118.
2 P. Bonhôte, A. Dias, N. Papageorgiou, K. Kalyanasundaram and M. Grätzel, *Inorg. Chem.*, 1996, **35**, 1168–1178.
3 Most recentlyA. Bradley, C. J. Cogan, B. C. Hanson, R. G. Lewin, M. D. Ogden, S. L. Owens, W. R. Pitner, D. W. Rooney, D. Sanders, N. G. Smart, R. Taylor, J. Richard, R. C. Thied, *PCT Int. Appl.*, 2002, pp. 26 WO 0266712; G. Francio, M. Solinas, E. Janssen, W. Leitner, A. Boesmann, P. Wasserscheid, J. Zimmermann, D. Ballivet-Tkatchenko, M. Picquet, S. Stutzmann, *PCT Int. Appl.*, 2002, pp. 29 WO 0292204; M. A. Klingshirn, G. A. Broker, J. D. Holbrey, K. H. Shaughnessy and R. D. Rogers, *Chem. Commun.*, 2002, 1394–1395.
4 G. M. Sheldrick, SHELXS-97, University of Gottingen, 1997.
5 G. M. Sheldrick, SHELXL-97, University of Gottingen, 1997.
6 J. Sun, D. R. MacFarlane and M. Forsyth, *Ionics*, 1997, **3**, 356–362.
7 J. Sun, M. Forsyth and D. R. MacFarlane, *Molten Salt Forum*, 1998, **5–6**, 585–588.
8 B. Helferich and H. Grünert, *Ber.*, 1940, **73B**, 1131–1133.
9 F. Runge, H. Engelbrecht and H. Franke, *Chem. Ber.*, 1955, **88**, 533–41.
10 A. Blaschette, E. Wieland, G. Seurig, D. Koch and F. Sarafi, *Z. Anor. Allg. Chem.*, 1983, **506**, 75–86.
11 D. R. MacFarlane, J. Sun, J. Golding, P Meakin and M. Forsyth, *Electrochim. Acta*, 2000, **45**, 1271–1278.
12 J. Huang, P. Chen, I. Sun and S. P. Wang, *Spectrosc. Lett.*, 2001, **34**(5), 591–603; C. J. Dymek, D. A. Grossie, A. V. Frantini and W. W. Adams, *J. Mol. Struct.*, 1989, **213**, 25–34.
13 J. Foropoulos. Jr and D. D. DesMarteau, *Inorg. Chem.*, 1984, **23**, 3720–3723.
14 C. M. Forsyth, D. R. MacFarlane, J. J. Golding, J. Huang, J. Sun and M. Forsyth, *Chem. Mater.*, 2002, **14**, 2103–2108.
15 O. Moers, K. Wijaya, D. Henschel, A. Blaschette and P. G. Jones, *Z. Z. Naturforsch., B*, 1999, **54**, 1420.
16 K. Baranyai, G. B. Deacon, D. R. MacFarlane, J. M. Pringle and J. L. Scott, *Aust. J. Chem.*, submitted.
17 J. O. Bockris and A. K. N Reddy, *Modern Electrochemistry*, Plenum Press, New York and London, 2nd edn., 1998, vol. 1.
18 A. J. McLean, M. J. Muldoon, C. M. Gordon and I. R. Dunkin, *Chem. Commun.*, 2002, **17**, 1880–1881.
19 W. Xu, E. L. Cooper and C. A. Angell, *J. Phys. Chem., B*, 2003, **107**, 6170–6178.
20 J. L. Anthony, E. J. Maginn and J. F. Brennecke, *J. Phys. Chem. B*, 2002, **106**, 7315–7320.
21 D. R. MacFarlane, P. Meakin, J. Sun, N. Amini and M. Forsyth, *J. Phys. Chem.*, 1999, **103**, 4164–4170.